Journal of Geochemical Exploration 243 (2022) 107104

Contents lists available at ScienceDirect

Journal of Geochemical Exploration

journal homepage: www.elsevier.com/locate/gexplo

Combining hydrogeochemistry, statistics and explorative mapping to estimate regional threshold values of trace elements in groundwater (Sardinia, Italy)

Elisabetta Dore [a], Riccardo Biddau [a], Mario Lorrai [b], Paolo Botti [b], Antonella Buccianti [c], Franco Frau [a], Rosa Cidu [a,*]

[a] Department of Chemical and Geological Sciences, University of Cagliari, Blocco A Monserrato, Italy
[b] Regione Autonoma della Sardegna-ADIS-Servizio tutela e gestione delle risorse idriche, via Mameli 88, 09100 Cagliari, Italy
[c] Department of Earth Sciences, University of Florence, Florence, Italy

ARTICLE INFO

Keywords:
Groundwater
Trace elements
Threshold values
Mapping
Compositional data analysis (CoDA)
Sardinia

ABSTRACT

Assessing geochemical baseline and threshold values of potentially toxic elements at adequate scales is fundamental for distinguishing geogenic contamination from anthropogenic pollution in groundwater. This study was aimed to estimate the regional threshold values of Li, Be, B, Al, V, Cr, Mn, Fe, Co, Ni, Cu, Zn, As, Se, Rb, Sr, Mo, Ag, Cd, Sb, Te, Ba, Hg, Tl, Pb, Bi, and U (elements listed according to atomic numbers) in groundwater, compare results to guidelines established for drinking water and the protection of groundwater from contamination, investigate the geographical distribution of trace elements, and assess the potential influence of water-rock interaction.

A pre-selection aimed at excluding groundwater samples affected by known anthropogenic activities was carefully carried out based on hydrogeochemical characteristics of waters and considering the potential sources of contamination. The resulting dataset was comprised of 1227 groundwater sampling sites located in Sardinia (Italy). Undetected values were treated using the Regression on Order Statistics method. For elements containing >75 % of undetected values and/or a limited number of samples in the dataset (Li, Rb, Sr, Mo, Ag, Te, Tl, Sb, Hg and Bi), the threshold values were estimated using either the 95th or 97.7th percentiles. For the other elements the mean + 2SD (Standard Deviation), the median + 2MAD (Median Absolute Deviation), and the TIF (Tukey Inner Fence) estimators were also calculated.

Geochemical maps allowed to recognize the threshold value of each element at different scales. Regional threshold values of the regulated elements B, Al, V, Cr, Cu and Cd in groundwater were below the Italian and World Health Organization drinking water guidelines, whereas Mn and As were above them. Regional threshold values estimated with TIF exceeded the drinking water guidelines for Ni, Se, Pb and U.

Results of this study showed that high concentrations of trace elements in groundwater were primarily dependent on the corresponding amount in parent materials with which the groundwater came into contact. Physical-chemical parameters and geochemical characteristics may contribute to enhancing concentrations of some trace elements in groundwater, e.g. As via reductive dissolution of Fe(III)-Mn(IV) hydroxides/oxides, Pb via formation of stable aqueous complexes, and other elements via adsorption onto fine particles with size below 0.4 μm (i.e. the pore size of filters used).

Maps drawn on the centered log-ratio (*clr*) transformation of hydrogeochemical data, following the CoDA (Compositional Data Analysis) approach, allowed to pinpoint critical areas to be investigated in more detail. For each geological complex, groundwater samples likely representing nearly pristine conditions were identified. The monitoring of these representative groundwater samples may help to pinpoint eventual changes in environmental conditions.

* Corresponding author.
E-mail address: cidur@unica.it (R. Cidu).

https://doi.org/10.1016/j.gexplo.2022.107104
Received 18 May 2022; Received in revised form 13 September 2022; Accepted 13 October 2022
Available online 19 October 2022

1. Introduction

Trace elements naturally occurring at parts per million levels in the Upper Continental Crust (Rudnick and Gao, 2014) are generally present at parts/sub-parts per billion concentrations in natural waters (Stumm and Morgan, 1996). The occurrence of trace elements in groundwater can be due either to natural sources, such as dissolution of minerals that come into contact with the water, or human activities, such as mining, fuel use, ore smelting and improper disposal of industrial and urban wastes (Appelo and Postma, 1993). Trace elements such as Mn, Fe, Co, Ni, Cu and Zn can be controlled by organic components, being essential micronutrients for biota within a defined range of concentrations (Lohan and Tagliabue, 2018). However, other elements such as Cr, As, Cd, Sb, Hg and Pb are known to be toxic to biota and high concentrations in groundwater may pose a threat to human health, as recognized by the World Health Organization (WHO, 2017). So, health-based targets should be established for the drinking water, as a part of overall water and health policy (WHO, 2017).

In some cases, toxic or harmful elements may occur in groundwater at high geogenic (natural) concentrations. It is the case of groundwater interacting with unexploited ore deposits and/or specific rock types, such as serpentinite (Binda et al., 2018), black shale (Parviainen and Loukola-Ruskeeniemi, 2019), and ultramafic rocks (Sahoo et al., 2019; Kierczak et al., 2021) that may be enriched in Ni, V, Cr, Cu, Zn and Mn. Therefore, it is essential to determine the geochemical baseline level (i.e. the actual background) of trace elements in groundwater with the aim to distinguish high concentrations due to natural sources (i.e., geogenic and biological processes) from contamination due to anthropogenic activities, such as urbanization, industrial activities, mining and agricultural practices. The threshold is the upper value of the baseline range calculated for each element, and is commonly used as a practical reference value to evaluate the *good* status of groundwater quality (Langmuir, 1997; Edmunds et al., 2003).

The best method of defining the geochemical baseline and the related threshold value is a matter of much discussion, and several approaches have been proposed (e.g.: Matschullat et al., 2000; Lee and Helsel, 2005; Reimann et al., 2005; Nordstrom, 2015; ISPRA, 2018; Reimann et al., 2018; Parrone et al., 2019; Zanotti et al., 2022). Methods include the calculation of percentiles of a given dataset (e.g.: 90th, 95th and 97.7th percentiles); the Median + 2 Median Absolute Deviations (MAD), the study of inflection points in a cumulative probability plot and the Tukey Inner Fence (TIF) estimator calculated as follows: 75th percentile + 1.5 IQR, where IQR is the interquartile range (75th–25th percentile). Because distributions of geochemical data are most often strongly right-skewed, in order to achieve a symmetrical (but not necessarily normal) data distribution, the correct approach would be to perform calculations on the logarithmic transformed data (Allegre and Lewin, 1995; Reimann et al., 2018; Gozzi et al., 2020). Moreover, the compositional nature of geochemical data is also to be taken into account and should be considered in statistical analysis of geochemical data (Buccianti and Grunsky, 2014; Boente et al., 2022).

The concentrations of substances dissolved in groundwater may vary considerably in space and time. A high variability in the chemistry of groundwater may occur locally, particularly in geological environments in which marked variations in lithology occur both laterally and at depth. These conditions pose difficulties in establishing the geochemical baseline at a variety of scales. It is not possible to recognize and understand changes in natural systems if the natural baseline range has never been documented and mapped (Zoback, 2001). Geochemical maps at the continental-scale have been published in the United States (Smith et al., 2014), Australia (Gray et al., 2019) and Europe (Reimann et al., 2014a,b). These datasets have been used to establish the geochemical baseline variation at the continental scale and, in Europe, for risk assessment of metals in the environment (e.g., Oorts and Schoeters, 2014; Birke et al., 2016).

In summary, for assessing the impact of contaminants on groundwater systems, and eventually establishing regulatory limits, and groundwater remediation programs, it is mandatory to know the baseline concentrations of contaminants at an adequate scale. This study was based on data acquired by hydrogeochemical investigations carried out in Sardinia (Italy). In this region, many areas are unaffected by diffuse anthropogenic pollution that allow to evaluate the present status of groundwater quality, possibly close to nearly pristine conditions. However, Sardinia hosts widespread mineralization, both mined and not exploited, which makes challenge the baseline evaluation of trace elements.

Specific objectives of this study were to: *i)* assess the regional occurrence of trace elements Li, Be, B, Al, V, Cr, Mn, Fe, Co, Ni, Cu, Zn, As, Se, Rb, Sr, Mo, Ag, Cd, Sb, Te, Ba, Hg, Tl, Pb, Bi, and U in Sardinian groundwater; *ii)* calculate the regional threshold values of trace elements using different estimators and compare results with guidelines established for drinking water and the protection of groundwater; *iii)* draw explorative maps for investigating the geographical distribution of trace elements, also considering the compositional data analysis (CoDA) approach; and *iv)* assess the potential influence of rock composition on concentrations of trace elements in groundwater.

2. Study area

The study area is located in Sardinia (Italy), an island extending 24,090 km^2 in the western Mediterranean Sea. Sardinia hosts 1,672,000 inhabitants mainly located in few cities (ISTAT, 2011). The average altitude is 334 m above sea level (asl). Mountains (19 % of land) with maximum elevation of 1834 m asl are mainly located in the eastern part. Hills (68 % of land) prevail over flat areas, such as the Campidano Plain and the river mouths. Forests (53 % of land), pastures and forages (43 % of land) represent semi-natural and poorly-developed rural areas. Industries are mainly located nearby the cost (Fig. 1), with limited influence on water bodies inland.

Sardinia is a remnant of continental crust developed during the Variscan Orogeny, characterized by a structural complexity due to the occurrence of significant geodynamic events from the post-collision Permian time up to the Oligocene-Miocene and Pliocene (Carmignani et al., 2015). Geological records can be summarized as follows: (a) the Paleozoic basement, mostly extending in the eastern part of the island, that underwent repeated phases of deformation and metamorphism during the Caledonian and Variscan orogenic cycles, and locally intruded by calc-alkaline granitic rocks; (b) the Mesozoic carbonate sequence that formed the passive margin of Southern Europe; and (c) the calc-alkaline volcanic rocks (Tertiary), alkaline basalts (Quaternary), and sedimentary cover consisting of shallow-water marine carbonates, siliciclastic sediments and continental conglomerates of Tertiary to Quaternary age (Carmignani et al., 2015).

Relevant regional faults (Fig. 1) are: Oligocene-Aquitanian ENE-WSW trending left lateral strike-slip faults that displace both granitic-metamorphic basement and Mesozoic-Tertiary sedimentary and volcanic sequences; middle-late Burdigalian NNW-SSE trending normal faults that define an assemblage of half-grabens, known as the Sardinia Rift (Funedda et al., 2000); and Plio-Pleistocene N-S trending extensional faults along which an anorogenic volcanic phase occurred (Paternoster et al., 2017).

Climatic conditions in Sardinia vary from semi-arid in the plain to semi-humid in the mountains. Average high, low and annual temperatures are 8 °C, 21 °C and 14.5 °C, respectively. The average precipitation is 764 mm (about 18 billion m^3/year) with rainy periods usually extending from November to April, but the intensity and length of the rainy season varies from year to year, with about 50 to 90 rainy days per year; heavy-rain events have been increased in the last decades (Delitala et al., 2000). The mean effective infiltration has been estimated at 940 Mm^3/year (RAS, 2006). However, the combined effect of temperature and winds on the island causes an inflow loss due to significant evapotranspiration. Hydrogeologic complexes with low ($<10^{-9}$ m/s) and

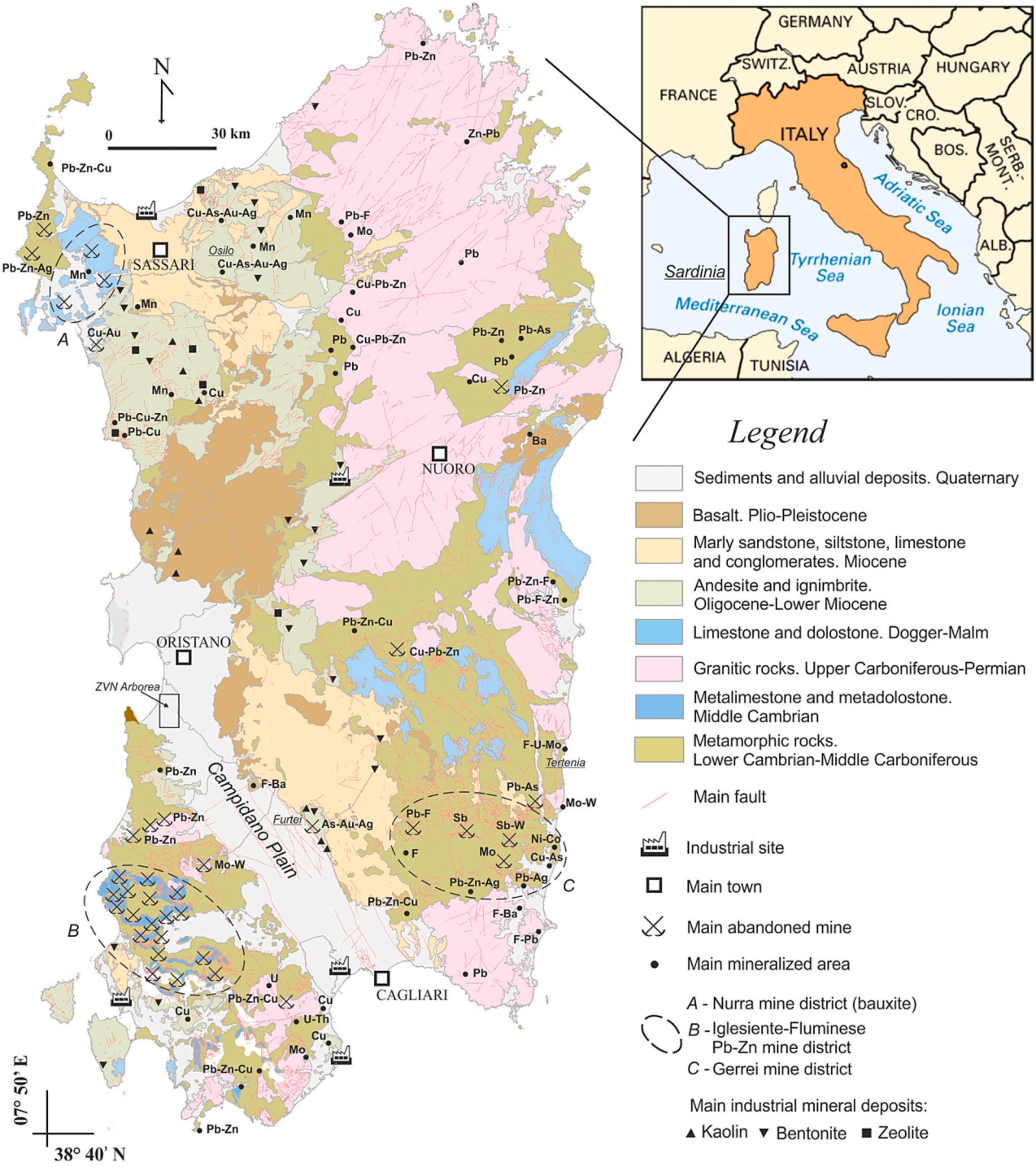

Fig. 1. Location of the study area and simplified geological map of Sardinia (modified after RAS, 2013) showing main industrial sites, mining districts, mineralized areas (De Vivo et al., 1998; Marcello et al., 2008) and relevant industrial mineral deposits (Palomba et al., 2006).

medium (10^{-9}–10^{-4} m/s) permeability cover about 60 % of the Sardinian territory, including Paleozoic granitic and metamorphic rocks, and Oligo-Miocene volcanic rocks (Ghiglieri et al., 2014). Water circulation in the Paleozoic metamorphic complex mostly occur in the upper fractured zones. In the granitic complex, aquifers may be found also in the weathered parts, that acquire a porous permeability, and dimensions may be limited by the presence of lamprophiric dikes, which act as underground barriers (Ghiglieri et al., 2014). Hydrogeologic complexes with good (10^{-4}–10^{-2} m/s) and high (>10^{-2} m/s) permeability represent about the 18 % of the land, consisting of Mesozoic and Cambrian limestone and dolostone, Quaternary alluvia and scoriaceous basalts (Ghiglieri et al., 2014). A simplified geological map of Sardinia showing the location of relevant mines, mineralized areas (Marcello et al., 2008; De Vivo et al., 1998; Palomba et al., 2006), and industrial sites is shown in Fig. 1. Sardinia was a relevant mining region in Italy and Europe, with Zn—Pb(Ag)—Cu—Ba—Sb exploitation carried out intensively since 1880 till 1990. Stratabound deposits are the more economic ores in Sardinia. They are often hosted in the Lower Paleozoic rocks in southwest Sardinia (Iglesiente-Fluminese, Fig. 1) where sphalerite-galena-barite large deposits may occur as massive sulfides

and small deposits as Mississippi Valley type (De Vivo et al., 1998; Moroni et al., 2019). In central and southeast Sardinia, stratabound mineralization consists of scheelite, arsenopyrite, antimonite (Gerrei, Fig. 1), and chalcopyrite-sphalerite-galena massive sulfides (Funedda et al., 2018). Some skarn deposits are connected to the granite intrusion (Naitza et al., 2017). Auriferous mineralization associated with sulfide minerals was discovered in Tertiary volcanic rocks, and a gold mine was active at Furtei (Fig. 1) in central Sardinia from 1997 to 2003 (Cidu et al., 2013, and references therein). Post-Variscan hydrothermal deposits with barite, fluorite, galena, antimonite and argentite were documented in the Tertenia area (Fig. 1, Lorrai and Mereu, 1999), bauxite in the Nurra (Mameli et al., 2007; Mongelli et al., 2021), and kaolin, bentonite and zeolite small deposits in several parts of the island (Palomba et al., 2006; Mormone and Piochi, 2020). Abandoned mines pose serious environmental hazards, due to the weathering of mining-related wastes dumped nearby the mines, and the presence of highly contaminated groundwater flowing out of adits (Cidu et al., 2009).

3. Methods

3.1. Data source

Records used in this study were derived from several hydrogeochemical surveys carried out at the University of Cagliari (UNICA, Biddau et al., 2017 and reference therein) and from the groundwater monitoring program established by the Sardinian Regional Government (RAS, 2011). The same sampling protocol and analytical methods were used over time, thus results of different surveys were combined in one dataset. Hydrogeochemical surveys at UNICA were focused either on mine areas for assessing the impact of mining on the water quality, or in nearly pristine areas for investigating water-rock interaction processes. Sampling density and measured chemical elements were dependent on specific objectives established in each survey, therefore, the distribution of groundwater samples in the region was not homogeneous. The RAS groundwater-monitoring program is a long-term activity aimed to identify temporal trends in groundwater quality at the regional scale. The RAS monitoring sites included fresh groundwater from relevant water bodies, groundwater in areas of environmental relevance (e.g. wetlands) and target areas at industrial sites. For this study, analyses derived from the RAS surveys carried out in winter and summer in 2016 were available. Results on physical-chemical parameters, major components, nitrogen species and fluoride were published elsewhere (Biddau et al., 2017, and reference therein).

As an attempt to assess the status of groundwater as close as possible to natural conditions, the whole dataset was carefully submitted to a pre-selection. The pre-selection criteria were based on the location of known anthropogenic activities that may have disturbed the natural condition, together with hydrogeochemical features of groundwater samples (such as concentrations of major components, nitrogen species and phosphate indicating anthropogenic inputs) and field evidences. In particular, groundwater located at/downstream of industrial sites, in the nitrate vulnerable zone (NVZ) of Arborea (Fig. 1; RAS, 2005), in areas affected by past-mining activities, and in coastal areas affected by the intrusion of modern seawater due to over-exploitation were excluded. Thermal waters characterized by 30 to 75 °C temperatures, and deep and long circulation time, were excluded. Waters collected at wells with unknown construction details, and waters showing calculated charge balance (Appelo and Postma, 1993) >5 % were also excluded. The dataset resulting from the pre-selection included 1227 sampling sites. Physical-chemical parameters and major chemical components have been reported elsewhere (Biddau et al., 2017).

Depending on specific objectives to be achieved in each survey, Li, Rb, Sr, Mo, Te, Tl and Bi were only determined at 192 (Te) to 376 (Sr) groundwater sampling sites. Elements Be, B, Al, V, Cr, Mn, Fe, Co, Ni, Cu, Zn, As, Se, Ag, Cd, Sb, Ba, Hg, Pb, and U were determined at 984 (V) to 1227 (B) groundwater sampling sites. Location of sampling sites is shown in the geochemical maps that will be presented later.

On the basis of physical-chemical parameters and chemical components, a careful interpretation of the geochemical data, coupled with hydrogeological information on the water bodies (RAS, 2011), made it possible to identify 9 groups of samples according with the geological complex with which the groundwater comes into contact: Quaternary sediment, Quaternary basalt, Tertiary sediment, Tertiary andesite, Tertiary ignimbrite, Mesozoic carbonate, Paleozoic granite, Paleozoic metamorphic, and Paleozoic carbonate.

3.2. Analytical protocols and data quality

The analytical protocol for trace elements can be summarized as follows. Spring waters were collected at the first outflow. Well waters were collected using a pump, following slow purging. On site, the water was filtered (0.4 μm pore size) into pre-cleaned, high-density polyethylene bottles, acidified immediately upon filtration to 1 % (v/v) HNO_3 supra pure, and stored refrigerated until analyses. Chemical analyses in the RAS groundwater-monitoring program were carried out at certified laboratories (RAS, 2011).

In surveys carried out at UNICA, elements B, Fe, Mn, Co, Cu, Zn, Sr, Cd and Ba were determined both by inductively coupled plasma optical emission spectrometry (ICP-OES, ARL 3520) and ICP mass spectrometry (ICP-MS, PerkinElmer ELAN5000 and ELAN DRC-e). Elements Be, Al, V, Cr, Co, Ni, Cu, Se, Ag, Cd, Sb, Ba, Pb, and U were determined by ICP-MS. The element Rh, 103 amu and 10 μg/L concentration, was used as internal standard in ICP-MS analyses. Elements As and Hg were determined by flow injection online with ICP-MS, hydride and vapor generation, respectively (Cidu, 1996).

For each analytical run, the detection limits (DL) were calculated at 10 times the standard deviation (SD) of the mean value calculated on several analyses of the blank solution, made up of ultrapure water MILLI-Q and supra pure HNO_3 1 % (v/v). It is worth to recall that the dataset for each element used in this study was generated over years. Because the DL may vary depending on instrument performance, different DL values resulted for each element.

In order to check potential contamination during sampling and analysis, blank solutions using MILLI-Q water were prepared in the field (field blank) and processed using the same procedures used for the water samples. Concentrations of trace elements in field blanks were either below or very close to the DL. Duplicated analyses showed concentration differences below 8 %. The standard reference solutions SRM1643d,e (supplied by the US National Institute of Standard & Technology, Gaithersburg, Maryland) and EnviroMAT ES-L-3 (supplied by SCP Science, St. Laurent, Quebec) were used to estimate analytical errors, which varied temporally depending on instrument performances. A few results showing measured concentrations versus certified values of standard reference solutions and the corresponding errors, usually below 10 %, are reported in the Supplementary material Table S1 and Table S2.

With reference to the evaluation of groundwater quality, the guidelines established by the WHO (2017) for drinking water and threshold values established by Italian legislations for drinking water and for the protection of groundwater (GURI, 2006, 2009, 2016) based on the European legislation (EC, 2006, 2014) were considered.

3.3. Statistical analysis

Several data-analysis procedures are available for datasets containing multiple detection limits (Lee and Helsel, 2005). For this study, concentrations below DL were processed as follows: *i)* for dataset containing undetected values below 5 % of samples, the detection limit was substituted with the detection limit itself (elements B, Rb, Sr, Ba, U); *ii)* for dataset containing from 6 % to 75 % of undetected values (elements Li, Be, Al, V, Cr, Mn, Fe, Co, Ni, Cu, Zn, As, Se, Mo, Cd, Pb), the detection limit was substituted using the Regression on Order Statistics method (ROS method, Shumway et al., 2002; Lee and Helsel, 2005); and *iii)* for

dataset containing >75 % of undetected values (elements Ag, Sb, Te, Hg, Tl, Bi) no substitution was made and the undetected values were disregarded. In general, if the information drawn from the variance-covariance matrix structure is sufficiently high, and cases are numerous, the method proposed by Martin-Fernandez et al. (2015) would be preferable. In our case, significant differences by the application of different methods were not observed.

Summary statistics were calculated after the DL substitution (with the exception of elements Ag, Sb, Te, Hg, Tl, and Bi having a large number of undetected values) and included the median value, selected percentiles, MAD and IQR. Histogram, cumulative probability plot and boxplot were used as exploratory data tools (Reimann et al., 2008; Filzmoser et al., 2009; Grunsky, 2010; Reimann and de Caritat, 2017; Sahoo et al., 2019).

Compositional data are closed (or constrained) data and it is not possible to interpret in a correct way the behavior of a single element without considering what occurs to all the others. The bias effect related to the compositional nature of geochemical data was taken into account for elements B, Al, Mn, Fe, Co, Ni, Cu, Zn, As, Cd, Ba, Pb and U (other elements were not considered due to a large number of undetected concentrations) using the centered log-ratio (*clr*) transformation (Aitchison, 1986) where for the composition $\mathbf{x} = (x_1, x_2, \ldots, x_D)$ with D components or variables is defined as:

$$clr(\mathbf{x}) = \left(log\frac{x_1}{g_m(\mathbf{x})}, log\frac{x_2}{g_m(\mathbf{x})}, \ldots, log\frac{x_D}{g_m(\mathbf{x})} \right)$$

where $g_m(\mathbf{x}) = \prod_{i=1}^{D} x_i^{1/D}$ is the geometric mean of the row.

In order to investigate multivariate relationships and potential correlations between chemical elements, the compositional *clr*-biplot was then performed (Daunis-I-Estadella et al., 2006; Pawlowsky-Glahn and Buccianti, 2011; Gozzi et al., 2020). The *clr*-transformation was also applied to draw maps of compositional data (hereafter *clr*-map). When a *clr*-map is adopted it is possible to have a whole framework of the variance-covariance structure of the dataset since the transformation takes into account, simultaneously, the link among all the elements of the composition. Thus, *clr*-maps represent a relative abundance and show whether the measured concentration of each element is high or low in relation to the geometric mean of all other elements (Reinmann et al., 2012).

The threshold values were calculated considering different estimators. For the elements containing <75 % of undetected values (Be, B, Al, V, Cr, Mn, Fe, Co, Ni, Cu, Zn, As, Se, Cd, Ba, Pb and U) the threshold values were calculated using: *i)* mean + 2SD (Standard Deviation), *ii)* median + 2MAD, *iii)* the TIF estimator, and *iv)* selected percentiles of the distribution (95th and 97.7th). Calculations were performed on the log-transformed data, then threshold values were obtained back-transforming the results. It should be noted that percentiles of the distribution are not influenced by the logarithmic transformation. For elements Li, Rb, Sr, and Mo, containing <75 % of undetected values but with a limited number of samples in the dataset, the threshold values were estimated using the percentiles of the distribution, either 95th or 97.7th. For elements Ag, Te, Tl, Sb, Hg and Bi, having a limited number of samples in the dataset and/or >75 % of undetected values, the threshold values were not calculated, but concentration maps were drawn.

Statistical analyses were accomplished with the free language for statistical computing R version 3.6 (R Development Core Team, 2013) and the package NADA (Nondetects And Data Analysis) was used for the ROS method. Also, the free open source CoDaPack software (Comas-Cufí and Thió-Henestrosa, 2011) was used to perform the *clr*-transformation of raw data and the *clr*-biplot.

The groundwater composition given by B, Al, Mn, Fe, Co, Ni, Cu, Zn, Ba and U was used for the searching of the "baseline composition". The robust Mahalanobis distance of each composition from the robust barycenter of a homogeneous group of data was determined following the approach reported in Verboven and Hubert (2005), after to have transformed the data in isometric coordinates (Egozcue et al., 2003). For each geological complex with which the groundwater comes into contact the distance-distance plot was obtained displaying robust distance (RD_i) versus classical Mahalanobis distance (MD_i). The horizontal and vertical lines in the RD_i-MD_i plot are drawn at the cut-off value:

$$\sqrt{\chi^2_{p,0.975}}$$

with p number of variables.

Geochemical concentration maps and *clr*-maps were drawn using ArcGIS 10.2 (ESRI, 2013).

4. Results

4.1. Summary statistics

The summary statistics of concentrations of trace elements is reported in Table 1, together with the drinking water guidelines established by the Italian Government and the WHO. Among the analyzed elements only Sr showed concentrations above DL in all samples. Elements Li, B, Cu, Zn, Rb, Ba and U showed <10 % of undetected values; V, Mn and Mo undetected concentrations were in the range of 21 to 49 %; Be, Al, Cr, Fe, Co, Ni, As, Se, Cd and Pb had 56 % to 72 % of undetected values; Ag, Sb, Te, Hg, Tl and Bi showed undetected values ranging from 86 % to 99 % (Table 1).

Among the regulated elements, the concentrations of Cr (maximum value 14 μg/L) and Ba (maximum value 486 μg/L) in the studied waters were always below guidelines (Table 1). The highest value of Cu (1380 μg/L) occurred in groundwater at one single sampling site; excluding that value, the maximum concentration of Cu measured was 116 μg/L, i.e. lower than the Italian and WHO guidelines (1000 and 2000 μg/L, respectively). Elements B, Al, V, Ni, Sb, Tl and U showed values above guidelines in <1.0 % of samples, whereas Mn, Fe, As, Se, Cd, Hg and Pb showed a percentage of values above guidelines in the range of 1.0 (Cd) to 9.2 % (Mn).

4.2. Element associations

The median concentration of Li, Be, B, Al, V, Cr, Mn, Fe, Co, Ni, Cu, Zn, As, Se, Rb, Sr, Cd, Ba, Pb and U, i.e. those elements having undetected values below 75 %, grouped by the geological complex with which groundwater samples come into contact, are reported in Table 2. As compared with regional values, relatively high median concentrations of Zn, Cd, Ba and Pb were observed in groundwater interacting with Paleozoic carbonate rocks (Table 2), likely reflecting the occurrence of relevant Cd-bearing sphalerite [(Zn,Cd)S], barite [$BaSO_4$] and galena [PbS] deposits (Boni et al., 1999), which location is shown in Fig. 1. Vanadium and Cr median concentrations were relatively high in groundwater interacting with the Quaternary basalt, indicating a lithological control on their concentration in groundwater, which was in agreement with literature records (Wright and Belitz, 2010).

Based on values reported in Table 2, a compositional *clr*-biplot was drawn in order to identify relevant element associations, which may indicate specific geochemical processes and/or particular geological environments. The resulting compositional biplot is shown in Fig. 2, in which the first two components describe about 82 % of the cumulative data set variability, thus indicating the presence of a strong variance-covariance structure.

The longest rays from the origin were for Quaternary basalt and Paleozoic carbonate (Fig. 2). This indicates that the ratio of concentration of these components to all others is responsible for most of the variability across all samples. The shortest ray from the origin was for the Tertiary sediment group, implying that the ratio of concentration of these components to all others was less variable. Different geochemical

Table 1
Summary statistics of trace elements, and physical-chemical parameters in Sardinian groundwater and guidelines for drinking water and the protection of groundwater from contamination. DL = detection limit. Min = minimum value. Max = maximum value. MAD = median absolute deviation. IQR = inter quartile range. n = number of samples. nc = not calculated due to a small number of detected values. ne = not established.

Element	Total	>DL	<DL	<DL	Min	Max	MAD	IQR	25th	Median	75th	80th	90th	95th	97.7th	99th	Guidelines µg/L		% above guideline[c]
	n	n	n	%	µg/L	µg/L	µg/L	µg/L	µg/L	µg/L	µg/L	µg/L	µg/L	µg/L	µg/L	µg/L	Italian[a]	WHO[b]	
Li	356	332	24	7	<5	840	7.2	15	3.4	7.4	18	21	38	78	150	301	ne	ne	nc
Be	1149	506	643	56	<0.01	2.1	0.07	0.2	0.03	0.07	0.2	0.2	0.4	0.6	0.91	1.5	ne	ne	nc
B	1227	1212	15	1	<8	1700	44	73	27	51	100	119	184	302	470	921	1000	2400	0.9
Al	1159	391	768	66	<0.01	5600	0.15	0.8	0.03	0.11	0.84	1.4	8.1	19	62	180	200	ne	0.9
V	984	776	208	21	<0.04	71	0.89	2	0.5	1	2.5	3.3	6.5	10	15	31	50	ne	0.3
Cr	1009	383	626	62	<0.2	14	0.3	0.9	0.13	0.28	1	1	2	2.3	3.7	5	50	50	0
Mn	1212	615	597	49	<0.5	4000	0.88	4.4	0.29	1	4.7	7	31	150	470	1492	50	ne	9.2
Fe	1200	393	807	67	<3	22,000	1.7	11	2.3	6.7	14	17	40	122	640	2949	200	ne	4
Co	1216	425	791	65	<0.01	59	0.04	0.09	0.03	0.06	0.11	0.13	0.3	0.71	3	8.1	ne	ne	nc
Ni	1174	465	709	60	<0.07	56	0.25	0.9	0.07	0.2	0.93	1	2	3.7	6.3	12	20	70	0.4
Cu	1152	1042	110	10	<0.2	1380	1.3	2.4	0.55	1.1	3	3.6	7	15	23	34	1000	2000	0
Zn	1029	966	63	6	<1.0	3200	12	23	2.5	9.2	25	33	76	191	420	772	ne	ne	nc
As	1182	396	786	66	<0.1	288	0.32	0.7	0.05	0.24	0.8	1	3	5	20	62	10	10	3.4
Se	1027	287	740	72	<0.5	89	0.62	1.8	0.2	0.54	2	2	3	4.7	7.8	16	10	40	1.8
Rb	339	333	6	2	<0.1	183	1.2	4.1	0.41	1	4.5	6.8	14	23	32	52	ne	ne	nc
Sr	376	376	0	0	20	14,000	123	197	73	150	270	315	653	1288	2000	3528	ne	ne	nc
Mo	320	198	122	38	<0.01	76	0.24	0.5	0.09	0.2	0.59	0.84	2	7.7	16	29	ne	ne	nc
Ag	1099	63	1036	94	<0.01	1.3	nc	nc	<0.04	<0.04	<0.04	<0.05	<0.1	0.12	0.27	1	ne	ne	nc
Cd	1136	262	874	72	<0.01	73	0.004	0.09	0.01	0.04	0.1	0.11	0.2	0.5	1.8	3.1	5	3	1
Sb	1173	170	1003	86	<0.04	24	nc	nc	<0.2	<0.2	<0.2	<0.3	0.6	1.1	2	2.3	5	20	0.7
Te	192	3	189	98	<0.03	0.5	nc	nc	<0.03	<0.06	<0.1	<0.4	<0.4	<0.5	<0.5	0.5	ne	ne	nc
Ba	1215	1191	24	2	<1.0	486	30	49	12	29	61	68	98	136	170	210	ne	1300	0
Hg	1037	108	929	90	<0.1	4.5	nc	nc	<0.1	<0.1	<0.1	<0.2	0.4	0.6	0.9	1.8	1	6	1.6
Tl	323	41	282	87	<0.01	5.9	nc	nc	<0.04	<0.05	<0.1	<0.2	0.35	0.4	0.5	0.78	2[d]	ne	0.9
Pb	1052	406	646	61	<0.04	80	0.08	0.4	0.028	0.1	0.39	0.6	1.1	2.5	7.1	19	10	10	1.8
Bi	280	3	277	99	<0.01	16	nc	nc	<0.04	<0.1	<0.3	<0.3	<0.6	<1.0	<1.0	2	ne	ne	nc
U	1171	1123	48	4	<0.01	151	1	1.9	0.22	0.77	2.1	2.6	5.7	11	19	29	ne	30[e]	0.9

Parameter	Total n	Unit	Min	Max	MAD	IQR	25th	Median	75th	80th	90th	95th	97.7th	99th
T	1227	°C	5.0	29.0	3.0	5.0	15	18	20	21	22	23	25	26
pH	1227		4.2	9.0	0.49	0.69	6.8	7.1	7.5	7.6	7.8	8.0	8.3	8.5
Eh	1178	V	0.03	0.77	0.05	0.23	0.16	0.19	0.39	0.43	0.47	0.48	0.49	0.51
EC	1227	mS/cm	0.10	9.4	0.67	0.99	0.57	0.94	1.6	1.8	2.4	3.2	4.3	5.6

[a] GURI, 2006, 2009, 2016.
[b] WHO, 2017.
[c] Lower guideline value was considered.
[d] Provisional guideline value IMH, 2016.
[e] Provisional guideline value WHO, 2017.

Table 2
Median concentrations (in μg/L) of trace elements in Sardinian groundwater at regional level and in groundwater grouped by geological complexes. nc = not calculated due to a small number of samples.

Element	Regional	Quaternary		Tertiary			Mesozoic	Paleozoic		
		Sediment	Basalt	Sediment	Andesite	Ignimbrite	Carbonate	Granite	Metamorphic	Carbonate
Li	7.4	nc	0.20	30	12	3.4	1.4	7.1	6.9	6.6
Be	0.07	0.10	0.006	0.10	0.06	0.049	0.015	0.05	0.06	0.02
B	50	82	32	74	58	44	38	25	21	48
Al	0.11	0.07	0.002	0.70	0.33	0.38	0.010	1.3	3.6	0.05
V	1.0	1.3	3.7	1.0	2.9	2.0	0.6	0.7	0.6	0.10
Cr	0.28	0.20	0.73	0.40	0.36	0.28	0.05	0.12	0.20	0.034
Mn	1.0	0.4	0.013	1.4	4.0	0.8	0.06	2.0	3.0	1.0
Fe	6.7	4.0	0.3	13	12	8.1	0.9	11	10	0.55
Co	0.06	0.04	0.005	0.11	0.10	0.07	0.012	0.020	0.09	0.008
Ni	0.20	0.10	0.008	0.3	0.9	0.18	0.025	0.34	0.9	0.02
Cu	1.1	2.0	1.0	1.0	1.0	1.0	1.0	0.7	1.0	1.5
Zn	9.2	8.9	1.6	7.0	11	8.6	3.6	9.9	21	50
As	0.24	0.15	0.005	0.6	0.3	1.8	0.022	0.04	0.6	0.011
Se	0.5	0.4	0.04	1.1	0.60	0.65	0.11	0.2	0.6	0.07
Rb	1.0	nc	1.9	10	7.6	3.8	0.5	0.4	0.8	1.8
Sr	150	nc	177	611	334	137	64	105	136	105
Mo	0.2	nc	0.30	1.1	0.20	0.30	0.14	0.2	0.3	0.06
Cd	0.04	0.029	0.002	0.09	0.051	0.061	0.006	0.012	0.1	0.11
Ba	29	49	19	30	18	16	16	12	18	73
Pb	0.10	0.04	0.003	0.15	0.12	0.080	0.009	0.16	0.11	1.0
U	0.8	1.0	0.3	1.4	0.4	0.8	0.7	0.9	0.2	0.7

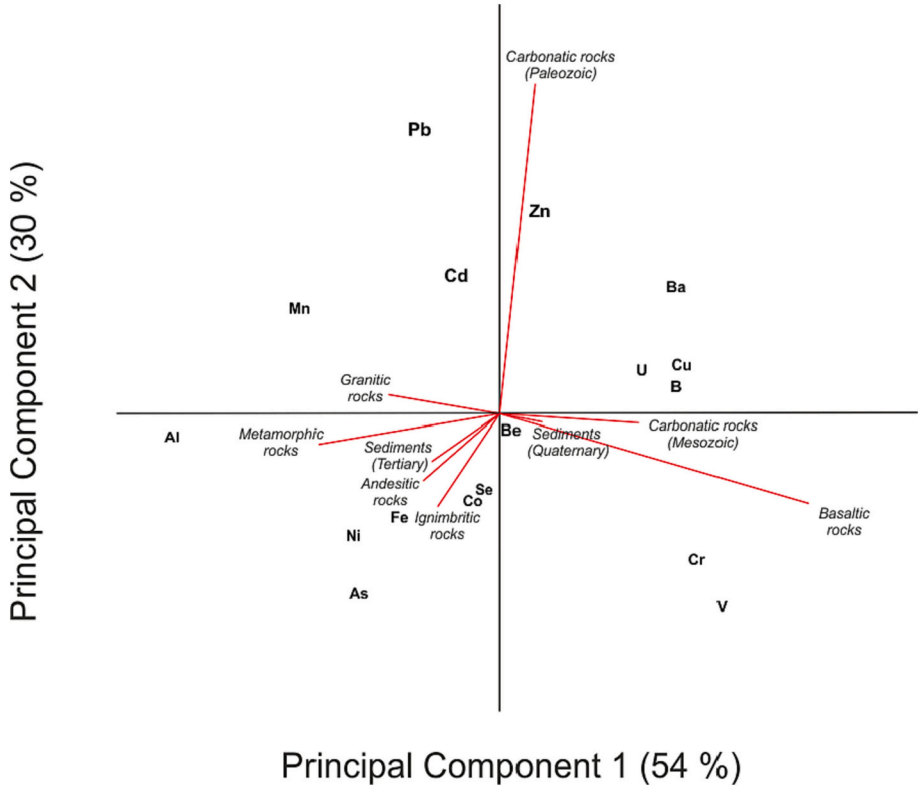

Fig. 2. Compositional *clr*-biplot showing the relationship among the median values of selected trace elements in groundwater samples grouped by the geological complexes. The principal component analysis was carried out on data reported in Table 2.

associations of elements with the geological complexes were observed. In particular, Zn, Cd and Pb were associated with the Paleozoic carbonate group (Fig. 2). Interesting in the biplot is the collinearity between basalt and granitic rock vectors revealing the presence of a subcomposition with a strong one-dimensional variability (Daunis-I-Estadella et al., 2006).

4.3. Regional threshold values

The threshold values calculated using different methods for Li, Be, B, Al, V, Cr, Mn, Fe, Co, Ni, Cu, Zn, As, Se, Rb, Sr, Mo, Cd, Ba, Pb and U in the Sardinian groundwater samples are reported in Table 3, together with guidelines established by the Italian Government and the WHO reported for comparison. The application of different estimators resulted in different threshold values. Threshold values calculated assuming the

Table 3
Threshold values (in μg/L) calculated using different estimators on the back transformed log-data. Drinking water guidelines are reported for comparison. MAD = median absolute deviation. SD = standard deviation. nc = not calculated due to a small number of samples. ne = not established. Values above the lower guideline are reported in bold.

Element	Back transformed ln-data					Guidelines	
	95th	Median + 2MAD	97.7th	Mean + 2SD	TIF	Italian[a]	WHO[b]
Li	78	nc	150	nc	nc	ne	ne
Be	0.6	1.3	0.9	1.0	4.0	ne	ne
B	302	366	470	435	719	1000	2400
Al	19	13	62	35	126	200	ne
V	10	11	15	16	28	50	ne
Cr	2.3	6.1	3.7	4.2	23	50	50
Mn	**150**	**61**	**470**	**181**	**302**	50	ne
Fe	122	87	**640**	200	192	200	ne
Co	0.7	1.0	3.0	1.1	2.0	ne	ne
Ni	3.7	9.3	6.3	7.2	**48**	20	70
Cu	15	11	23	20	37	1000	2000
Zn	191	282	420	350	814	ne	ne
As	5.0	**16**	**20**	**15**	**46**	10	10
Se	4.7	10	7.8	10	**62**	10	40
Rb	23	nc	32	nc	nc	ne	ne
Sr	1288	nc	2000	nc	nc	ne	ne
Mo	7.7	nc	16	nc	nc	ne	ne
Cd	0.5	0.6	1.8	0.8	1.9	5	3
Ba	136	313	170	245	691	ne	1300
Pb	2.5	4.3	7.1	5.3	**21**	10	10
U	11	20	19	24	**62**	ne	30

[a] GURI, 2006, 2009, 2016.
[b] WHO, 2017.

95th percentile provided the most conservative estimate. Threshold values calculated by the 97.7th percentile, the Mean + 2SD and the Median + 2MAD were within the same order of magnitude. The TIF method usually provided the highest threshold values, generally higher than the 97.7th value, except for Mn and Fe that showed many outliers.

For elements Li, Rb, Sr, and Mo the threshold values corresponding to 95th and 97.7th value of distribution, might be assumed as a provisional threshold estimate due to the small number of data available. The regional threshold values of the regulated elements B, Al, V, Cr, Cu and Cd, whatever the method used, were below the Italian and WHO drinking water guidelines. All calculated threshold values for Mn were higher than the Italian guideline value of 50 μg/L. Although Mn is not suspected of causing direct health effects through its presence in drinking water, high concentrations should be considered because may result in severe discoloration of water, and frequently may cause operational problems (WHO, 2017). The regional threshold values of As were mostly above the Italian and WHO drinking water guidelines. The regional threshold values calculated by TIF for Ni, Se, Pb and U exceeded the respective guidelines (Table 3).

5. Discussion

Elements As, Cd and Pb are discussed first due to: *i)* their high toxicity to human health; *ii)* the widespread mineral deposits hosting these elements in Sardinia; and *iii)* detectable concentrations sufficient to draw both concentration maps and *clr*-maps, which are included in the main text. Other elements were grouped based on the availability of detected concentrations, with maps provided in the Supplementary Figs. S1, S2 and S3.

5.1. As, Cd and Pb

Elements As, Cd and Pb hosted in sulfide minerals can be dissolved under oxidizing conditions. Schematic reactions of arsenopyrite [FeAsS], enargite [Cu_3AsS_4], sphalerite [(Zn,Cd)S] and galena [PbS] dissolution are showed in Eqs. 1, 2, 3 and 4, respectively (Plumlee, 1999; Dold, 2010; Cidu et al., 2018):

$$4FeAsS + 13O_2 + 6H_2O \rightarrow 4Fe^{2+} + 4H_2AsO_4^- + 4SO_4^{2-} + 4H^+ \quad (1)$$

$$Cu_3AsS_4 + 8.75O_2 + 2.5H_2O \rightarrow 3Cu^{2+} + AsO_4^{3-} + 4SO_4^{2-} + 5H^+ \quad (2)$$

$$\left(Zn_{(1-x)}Cd_x\right)S + 2O_2 \rightarrow (1-x)Zn^{2+} + xCd^{2+} + SO_4^{2-} \quad (3)$$

$$PbS + 2O_2 \rightarrow Pb^{2+} + SO_4^{2-} \quad (4)$$

The above reactions are fundamental for understanding the occurrence of As, Cd and Pb in the studied groundwater samples. Fig. 3 shows the maps of As, Cd and Pb concentrations, with symbol sizes corresponding to the threshold value calculated using different estimators based on the log-transformed data. High concentrations of As in groundwater (Fig. 3a) were related to the oxidative dissolution of arsenopyrite and enargite mineralization hosted in Tertiary volcanic rocks, respectively in the north (Osilo; Biddau and Cidu, 2005) and central (Furtei; Cidu et al., 2013) Sardinia, and to the diffuse occurrence of arsenopyrite in metamorphic rocks in southeast Sardinia (Fig. 1, Gerrei; Frau et al., 2012).

Elevated Cd concentrations in groundwater were observed in south Sardinia (Fig. 3b), mostly related to the interaction of water with Cd-bearing sphalerite mineralization (Cidu et al., 2009). The Pb map (Fig. 3c) showed relatively high concentrations in groundwater draining the Iglesiente-Fluminese mining districts that host relevant galena deposits (Fig. 1). These finding were in agreement with the geochemical associations of Cd and Pb with the Paleozoic carbonate rocks shown in the bi-plot (Fig. 2).

Fig. 4 shows the maps of As, Cd and Pb derived from the *clr*-data, representing the relative abundance of each element with respect to the geometric mean of all elements considered. In addition to the areas highlighted in the As concentration map (Fig. 3a), the *clr*-As map allowed to identify relatively high concentrations of As also in areas where mineral deposits are not documented. In particular, in northern Sardinia a relative enrichment of As in groundwater was associated with Tertiary andesite and ignimbrite (Fig. 4a) that may host disseminate As-bearing sulfide minerals (Simeone et al., 2005). Another As cluster was observed in groundwater draining Quaternary sediments (Fig. 4a), close to Oristano (location shown in Fig. 1). In this flat area alluvia and

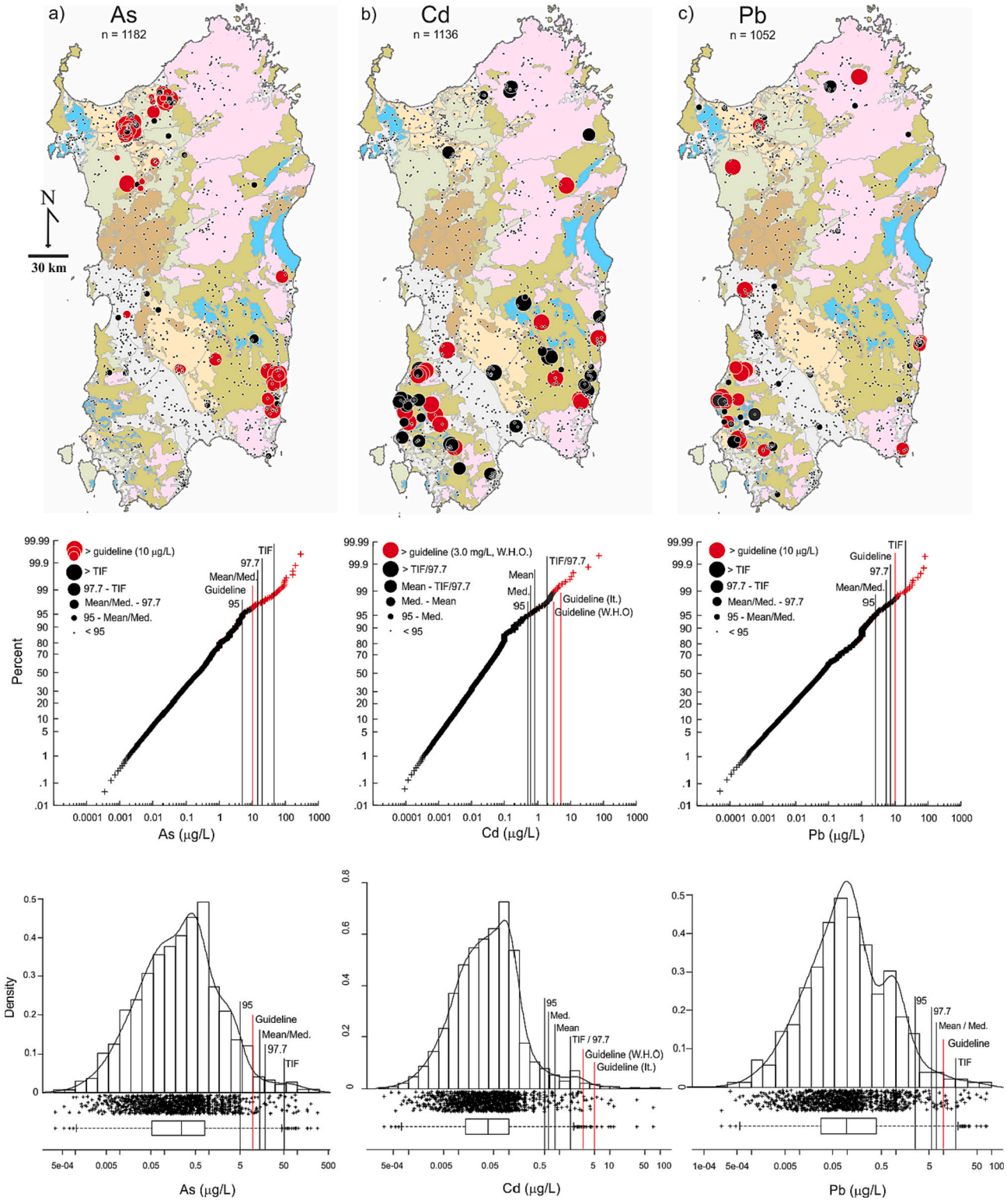

Fig. 3. Maps of As (a), Cd (b) and Pb (c) in Sardinian groundwater showing threshold values calculated with different methods based on the log-transformed data. The cumulative probability plot, histogram and boxplot are also reported for each element. Red symbols in the maps and cumulative plots indicate concentrations above guidelines. (For interpretation of the references to color in this figure legend, the reader is referred to the web version of this article.)

lacustrine sediments are often rich in organic matter that may promote reductive dissolution of Fe(III) and Mn(IV) hydroxides/oxides, according with the schematic reactions 5 and 6, which in turn would also release sorbed As into solution (Frau et al., 2019).

$$CH_2O + 4Fe(OH)_3 + 7H^+ \rightarrow 4Fe^{2+} + HCO_3^- + 10H_2O \quad (5)$$

$$CH_2O + 2MnO_2 + 3H^+ \rightarrow 2Mn^{2+} + HCO_3^- + 2H_2O \quad (6)$$

The *clr*-Cd (Fig. 4b) and *clr*-Pb (Fig. 4c) maps were similar to those drawn using concentration values, probably due to the prevalent association of these elements with widespread mineralization of Zn(Cd) and Pb in Sardinia, which is in agreement with literature records (Cidu et al.,

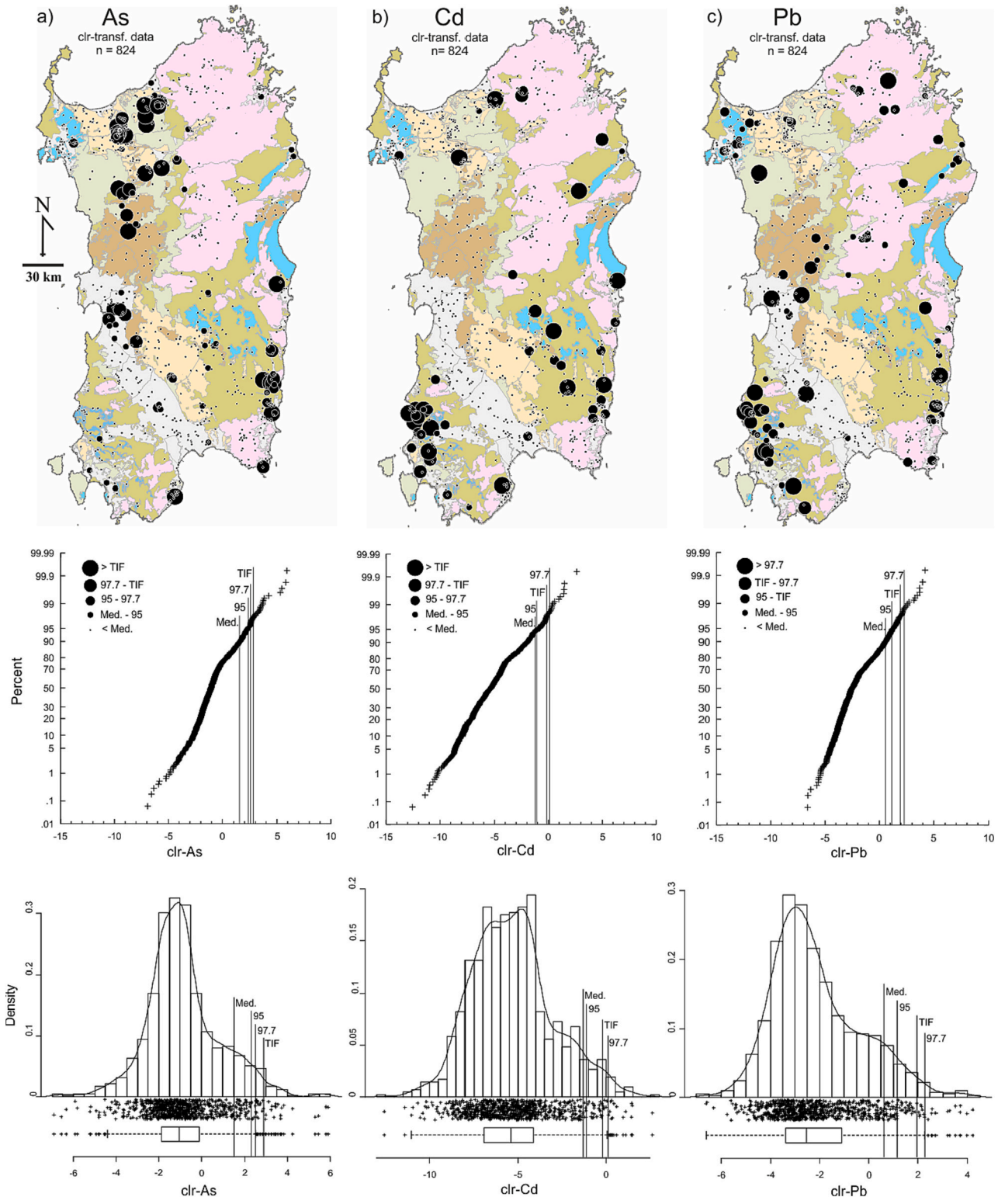

Fig. 4. Maps of As (a), Cd (b) and Pb (c) in Sardinian groundwater showing ranges of values calculated on the *clr*-transformed data. Symbol sizes in the maps increase as relative concentrations of each element with respect to all other components in groundwater increase. The cumulative probability plot, histogram and boxplot are also reported for each element.

2009). A small cluster with relatively high Pb was observed in groundwater circulating in Mesozoic carbonate rocks in northwest Sardinia (Fig. 4c). In such environment, the formation of complexes such as aqueous $PbCO_3^0$ is favored, which in turn would allow Pb to remain in groundwater due to the stability of this complex (Stumm and Morgan, 1996) under the near-neutral to slightly alkaline pH in groundwater of this area observed in this study and in literature (Da Pelo et al., 2017).

5.2. *B, Al, Mn, Fe, Co, Ni, Cu, Zn, Ba and U*

Concentration maps and *clr*-maps for elements B, Al, Mn, Fe, Co, Ni, Cu, Zn, Ba and U, together with the cumulative plot, histogram and

boxplot, are shown in the Supplementary Fig. S1.

The regional distributions of B showed high concentrations in groundwater interacting with marine-derived sediments of Miocene age (Fig. S1a), which is consistent with relatively high B in seawater (Stumm and Morgan, 1996). The *clr*-B map also showed groundwater interacting with basalt and andesite to be relatively enriched in B (Fig. S1b), which appears consistent with B enrichment in volcanic rocks that underwent hydrothermal alteration (Ryan and Langmuir, 1993).

About 1 % of total groundwater samples had Al concentrations above drinking water guidelines. High concentrations of Al were associated with pH values ranging from 4.2 to 5.5 observed in groundwater draining mineralized areas, such as Osilo and Furtei (Fig. S1c), which is consistent with increasing solubility of Al at pH < 6 (Stumm and Morgan, 1996). High concentrations of Al might be also associated with particles <0.4 μm in size, to which Al would be sorbed. Relatively high concentrations of Al (Fig. S1d) were observed in volcanic, granitic and metamorphic rocks, i.e. in silicate environments where Al is a major component.

Concentrations of Mn and Fe above guidelines were observed in 9.2 % and 4 % of total samples, respectively (Table 1). Maps of Mn (Fig. S1e, f) and Fe (Fig. S1g, h) in groundwater showed associations with different geological complexes, which appeared to be consistent with the diffused Mn and Fe abundance in Sardinian rocks (Sinisi et al., 2012), as well as in the Crust (Rudnick and Gao, 2014). The ion Mn^{2+} is stable under wide pH and redox range observed in natural waters (Stumm and Morgan, 1996), and in our samples (Table 1), which may account for the widespread high concentrations of Mn in the Sardinian groundwater. Also considering that Mn guideline was not established by WHO, the Italian guideline of 50 μg/L Mn appears probably inadequate for representing natural conditions, and establishing the *good* status of groundwater.

Relatively high Co (Fig. S1i, j), Ni (Fig. S1k, l) and Cu (Fig. S1m, n) in groundwater appeared often unrelated to specific rocks. Occurrence of Zn in groundwater (Fig. S1o, p) was often observed in the Iglesiente-Fluminese Zn—Pb mine districts (Fig. 1). Relatively high concentrations of Ba were observed in groundwater interacting with kaolin deposits (Fig. S1r), which would be consistent with literature records (Dill et al., 1995). High concentrations of Ba sometimes occurred in groundwater having low sulfate (not shown), highlighting the role of barite equilibrium in controlling aqueous Ba concentrations.

The highest concentrations of U were observed in oxic groundwater draining granitic environments (Fig. S1s), as expected considering the U content in granite higher than mafic rocks, and the U mobility as ion uranyl (UO_2^{2+}) and its complexes under oxic conditions (Campbell et al., 2015). However, the median value of U in groundwater draining granitic rocks was close to the regional value (see Table 2), suggesting that high U concentrations in groundwater might derive from interaction with U mineralization, such as in SW Sardinia (Fig. 1).

5.3. Li, Be, V, Cr, Se, Rb, Sr and Mo

Concentration maps for elements Li, Be, V, Cr, Se, Rb, Sr and Mo in Sardinian groundwater, together with the cumulative plot, histogram and boxplot, are reported in the Supplementary Fig. S2. Variations in concentrations of Li, Rb, Sr and Mo were found dependent on the interaction of groundwater with specific rocks. The highest concentrations of Li, Rb and Sr (Fig. S2a, f, g, respectively) were mainly observed in groundwater interacting with Tertiary andesite and ignimbrite that underwent hydrothermal alteration (Biddau and Cidu, 2005; Mormone and Piochi, 2020). Few spots with high Be and Cr occurred in groundwater draining granitic rocks (Fig. S1b and d, respectively), probably due to associated pegmatite. The maps of V and Cr (Fig. S2c, d, respectively) showed high concentrations mostly in groundwater draining Quaternary basalt, Tertiary andesite and ignimbrite in northwest Sardinia, which was in agreement with relatively high V and Cr contents reported in these rocks (Lustrino et al., 2013). Concentrations of Se above guidelines were observed in 1.8 % of total samples (Table 1), mostly associated with groundwater draining Quaternary and Tertiary sediments (Fig. S1e), for which the Se abundance is unknown. Concentrations of Mo (Fig. S2h) above the 97.7th threshold occurred in groundwater draining areas hosting known mineralization (e.g. the Gerrei district shown in Fig. 1; Cidu et al., 2021).

5.4. Ag, Sb, Te, Hg, Tl, and Bi

Concentration maps for these elements, together with the cumulative curve and box plot, are reported in the Supplementary Fig. S3.

Relatively high concentrations of Ag and Sb occurred in areas of known mineralization (e.g. Osilo, Iglesiente-Fluminese, Gerrei, Tertenia; see Fig. 1 for location). Concentrations above the Italian drinking water limit of 5 μg/L Sb were observed in 0.7 % of total samples (Table 1). Mercury concentrations above the drinking water limit of 1 μg/L (1.6 % of total samples, Table 1) occurred in areas of known mineralization (Fig. S3d). Indeed, Hg in the Iglesiente-Fluminese mining district was enough abundant to be recovered as byproduct from galena ore (Cidu et al., 2001). High concentrations of Hg were also found in groundwater in the Campidano Plain, and nearby urban areas (Fig. S3d). Such concentrations were apparently unrelated with geogenic processes. Therefore, these areas should be investigated in more detail to pinpoint eventual anthropogenic inputs. Concentrations of Te and Bi above DL occurred in 3 groundwater samples only (Fig. S3c, f, respectively).

Concentrations of Tl were below 0.7 μg/L in 99 % of total samples. The 3 samples with Tl concentrations slightly above the Italian guideline occurred in groundwater located nearby the mineralized area of Osilo and in granitic rocks of southern Sardinia (Fig. S3e). High concentrations of Tl were not related with high concentrations of U. More sampling sites would be required to assess the regional occurrence of Tl above the guideline of 2 μg/L. Being a regulated element, we suggest that the determination of Tl should be included in the groundwater monitoring program established by the Regional and National Governments.

5.5. Groundwater 'baseline composition'

The information obtained with the *clr*-maps allowed to further improve, under CoDA principles, the searching of the 'baseline composition', thus abandoning single elements and considering the fundamental links of the chemical species in the composition to which they pertain. The composition given by B, Al, Mn, Fe, Co, Ni, Cu, Zn, Ba and U in groundwater was used for this purpose. An example for groundwater samples interacting with the Paleozoic metamorphic rocks is reported in Fig. 5. Data located in the upper right quadrant were related to outliers or extreme compositions, whereas those located toward the down left corner were near to the robust barycenter. In the case of groundwater interacting with metamorphic rocks, the most extreme compositions were given by groundwater samples located downstream of known mineralization, which is consistent with high concentrations of trace elements due to the interaction of groundwater with the ore deposits. The composition closer to the robust barycenter in Fig. 5 was given by the spring sample N45 that was located far away either from known mineralization or anthropogenic activities, thus, likely close to nearly pristine environmental conditions.

The application of the analysis to the different geological complexes has allowed to identify the composition of groundwater samples closer to the compositional barycenter. These samples are listed in Table 4, with locations shown in the Supplementary Fig. S4. The Robust Mahalanobis distance (RD_i) threshold value separating anomalous or extreme compositions from the rest of the data for each geological complex is also reported in Table 4. The RD_i threshold values correspond to the horizontal red line in the distance-distance plots drawn for groundwater interacting with the different geological complexes, reported in the Supplementary Fig. S5. The composition of the groundwater samples listed in Table 4, characterized by joint relationships among B, Al, Mn,

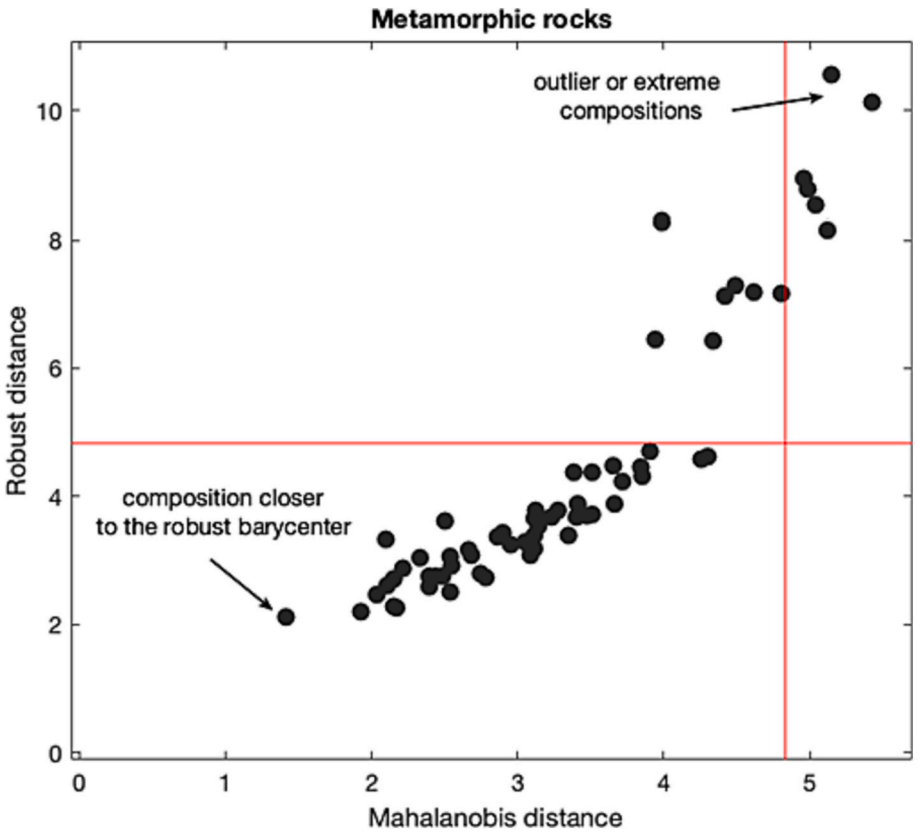

Fig. 5. Robust Mahalanobis distance versus classical distance for groundwater samples interacting with metamorphic rocks for the multivariate dataset given by B, Al, Mn, Fe, Co, Ni, Cu, Zn, Ba and U.

Table 4
Robust Mahalanobis distance (RD_i values) from the compositional barycenter of the dataset given by B, Al, Mn, Fe, Co, Ni, Cu, Zn, Ba and U, with groundwater samples listed for geological complexes ranked by age. The column on the right reports the RD_i threshold values separating outliers or extreme compositions.

Sample	Geological complex	RD_i values	RD_i threshold values
13101PO0028 — well	Quaternary	1.85	4.9
17104PO0004 — well	sediment	1.84	
22101SO0001 — spring	Quaternary basalt	1.31	5.1
23101PO0059 — well	Tertiary sediment	1.51	5.1
27203PO0004 — well	Tertiary ignimbrite	1.82	4.2
31101PO0006 — well	Tertiary andesite	1.98	4.85
34101SO0005 — spring	Mesozoic carbonate	1.29	8.2
N13 — spring	Paleozoic granite	1.83	4.9
N17 — spring		1.92	
BG1 — well	Paleozoic carbonate	1.33	4.9
37101PO0003 — well		1.59	
N45 — spring	Metamorphic rocks	1.92	4.7

Fe, Co, Ni, Cu, Zn, Ba and U, might represent the *baseline condition* of groundwater interacting with a specific geological complex. These samples could be considered as a reference in groundwater monitoring plans at different scales. Perturbations eventually observed in the reference groundwater sample under monitoring programs might give interesting early warning signals about environmental changes.

6. Conclusions

Establishing the actual natural quantification of aqueous components is mandatory to identify significant and feasible clean-up goals (European Water Framework Directive 2000/60/EC, article 17). The application of remediation strategies, simply following compliance levels established by current regulations, might lead to ineffective and unaffordable targets at sites where specific natural conditions may cause geogenic contamination of water systems. Following the assessment of contamination status with respect to baseline conditions at contaminated sites, remediation actions might be better planned by National and Regional Governments.

In this study, the calculated threshold values of trace elements may contribute to assess the quality of Sardinian groundwater. Prior to threshold calculations, an accurate pre-selection should be carried out before data processing, and samples affected by anthropogenic activities should be excluded. To this purpose, hydrogeochemical interpretations of data was a valuable tool in highlighting interactions of water with solid and gas phases, better predicting relations among elements, and recognizing anthropogenic effects. Also, selecting the reliable variables to be used on data processing was mandatory.

Based on geochemical maps, the most conservative threshold corresponded with values derived by the 95th percentile estimator. The 97.7th percentile, the mean + 2SD, the median + 2MAD, and the TIF estimators provided higher threshold values that should be considered at the local scale. Elements Mn, Fe, Ni, As, Se, Pb and U in groundwater showed threshold values above guidelines established for drinking water.

Concentrations of As, Zn, Cd, Sb and Pb above the threshold values mainly occurred in groundwater draining areas of known mineralization (see Fig. 1), highlighting the relevant role of element abundance in parent rocks and sediments with which the groundwater interacts. Elements Zn, Cd and Pb in groundwater showed a strong association with the Paleozoic carbonate formations that host relevant Zn(Cd)—Pb deposits. Long time mining in the Iglesiente-Fluminese Zn—Pb districts may have enhanced the availability of Zn, Cd and Pb via widespread

mining-derived wastes that have exposed larger surfaces to weathering, with respect to the surface of unexploited deposits.

The geochemical characteristics of groundwater showed that high concentrations and outliers values of trace elements were mostly associated to groundwater interacting with rocks enriched in specific elements and/or with mineral deposits. In addition to the geogenic abundance of trace elements, physical-chemical parameters and hydrogeochemical characteristics may contribute in enhancing concentrations in groundwater, e.g. via reductive dissolution driven by organic matter (As), the formation of stable aqueous complexes (Pb), equilibrium with respect to solid phases (Ba), without neglecting the role of colloidal and/or very fine particles as potential sorption sites for elements such as Al, Mn, Fe and As.

Both concentration maps and *clr*-maps are useful to understand the processes governing the spatial distribution of trace elements in groundwater. Compared with concentration maps, the use of *clr*-maps permitted to constrain the element source, giving a more complete picture of the behavior of each element with respect to other components in groundwater. The *clr*-maps were particularly useful to pinpoint critical areas to be investigated in more detail. In such areas, groundwater sampling and analyses should be implemented for better understanding ongoing processes and pinpoint potential sources of groundwater contamination. In fact, the *clr*-data spatial distribution might reveal decoupling phenomena of some elements with respect to the expected geochemical behavior, thus revealing unknown inputs or perturbations.

In this framework, the CoDA processing, able to recognize extreme compositions with respect to those closer to the compositional barycenter, can give a substantial contribution to recognize processes at the base of anomalous behavior of trace elements in groundwater, as well as more representative, perhaps pristine and/or stable, conditions.

The methodology adopted in this study appears adequate to distinguish effective anthropogenic contamination from natural conditions. Therefore, results of this study may help stakeholders to define realistic environmental clean-up goals, and consequently planning adequate strategies to reduce groundwater contamination at specific areas. The peculiarity of Sardinia, where varied mineral occurrences are widespread in the island (Marcello et al., 2008), should be also considered. Indeed, a common feature among the considered trace elements was that concentrations in groundwater increased depending on the geological availability in rocks hosting the water bodies. In addition to the geological abundance, specific conditions may play a significant role in enhancing the geochemical mobilization and spatial distribution of trace elements. As reported in the recent 2022 IPCC report (https://www.ipcc.ch/report/ar6/wg2/) climate change is causing substantial damages and increasingly irreversible losses in terrestrial freshwater at different scales, so that any investigation of the baseline of a Country represents a fundamental starting point to evaluate and quantify resilience of ecosystems and human communities.

Supplementary data to this article can be found online at https://doi.org/10.1016/j.gexplo.2022.107104.

Declaration of competing interest

Funds by the Regione Autonoma della Sardegna (Cooperation Agreement between DSCG-UNICA and RAS-ADIS-STGRI, CIG Z552D570E8) given to the Corresponding author R. Cidu were used for research purpose only, excluding any benefit derived from employment, consultancies, stock ownership, honoraria, paid expert testimony, patent applications/registrations.

Data availability

Data will be made available on request.

Acknowledgements

Research funded by the Regione Autonoma della Sardegna (Cooperation Agreement between DSCG-UNICA and RAS-ADIS-STGRI, CIG Z552D570E8, scientific responsible R. Cidu). Authors thank the Editor Prof. Stefano Albanese, the reviewer Dr. Ariadne Argyraki and an anonymous reviewer for their useful comments and suggestions.

References

Aitchison, J., 1986. The Statistical Analysis of Compositional Data. Chapman & Hall, London, pp 416.
Allègre, C.J., Lewin, E., 1995. Scaling laws and geochemical distributions. Earth Planet. Sci. Lett. 132, 1–13.
Appelo, C.A.J., Postma, D., 1993. Geochemistry, groundwater and pollution. In: 2nd edition. Balkema, Rotterdam, A.A, p. 536.
Biddau, R., Cidu, R., 2005. Hydrogeochemical baseline studies prior to gold mining: a case study in Sardinia (Italy). J. Geochem. Explor. 86, 61–85.
Biddau, R., Cidu, R., Lorrai, M., Mulas, M.G., 2017. Assessing background values of chloride, sulfate and fluoride in groundwater: a geochemical-statistical approach at a regional scale. J. Geochem. Explor. 181, 243–255.
Binda, G., Pozzi, A., Livio, F., Piasini, P., Zhang, C., 2018. Anomalously high concentration of Ni as sulphide phase in sediment and in water of a mountain catchment with serpentinite bedrock. J. Geochem. Explor. 190, 58–68.
Birke, M., Reimann, C., Oorts, K., Rauch, U., Demetriades, A., Dinelli, E., Ladenberger, A., Halamic, J., Gosar, M., Jähne-Klingberg, F., G.E.M.A.S. Project Team., 2016. Use of GEMAS data for risk assessment of cadmium in European agricultural and grazing land soil under the REACH regulation. Sci. Total Environ. 74, 109–121.
Boente, C., Albuquerque, M.T.D., Gallego, J.R., Pawlowsky-Glahn, V., Egozcue, J.J., 2022. Compositional baseline assessments to adress soil pollution. An application in Langreso, Spain. Sci. Total Environ. 812, 15383.
Boni, M., Costabile, S., De Vivo, B., Gasparrini, M., 1999. Potential environmental hazard in the mining district of southern Iglesiente (SW Sardinia, Italy). J. Geochem. Explor. 67, 417–430.
Buccianti, A., Grunsky, E., 2014. Compositional data analysis in geochemistry: are we sure to see what really occurs during natural processes. J. Geochem. Explor. 141, 1–5.
Campbell, K.M., Gallegos, T.J., Landa, E.R., 2015. Biogeochemical aspects of uranium mineralization, mining, milling, and remediation. Appl. Geochem. 57, 206–235.
Carmignani, L., Oggiano, G., Funedda, A., Conti, P., Pasci, S., 2015. The geological map of sardinia (Italy) at 1:250,000 scale. J. Maps 12, 826–835.
Cidu, R., 1996. Inductively coupled plasma - mass spectrometry and - optical emission spectrometry determination of trace elements in water. At. Spectrosc. 17, 155–162.
Cidu, R., Biagini, C., Fanfani, L., La Ruffa, G., Marras, I., 2001. Mine closure at Monteponi (Italy): effect of the cessation of dewatering on the quality of shallow groundwater. Appl. Geochem. 16, 489–502.
Cidu, R., Biddau, R., Fanfani, L., 2009. Impact of past mining activity on the quality of groundwater in SW Sardinia (Italy). J. Geochem. Explor. 100, 125–132.
Cidu, R., Biddau, R., Frau, F., Wanty, R.B., Naitza, S., 2021. Regional occurrence of aqueous tungsten and relations with antimony, arsenic and molybdenum concentrations (Sardinia, Italy). J. Geochem. Explor. 229, 106846.
Cidu, R., Da Pelo, S., Frau, F., 2013. Legacy of cyanide and ARD at a low-scale gold mine (Furtei, Italy). Mine Water Environ. 32, 74–83.
Cidu, R., Dore, E., Biddau, R., Nordstrom, D.K., 2018. Fate of antimony and arsenic in contaminated waters at the abandoned Su Suergiu mine (Sardinia, Italy). Mine Water Environ. 37, 151–165.
Comas-Cufí, M., Thió-Henestrosa, S., 2011. CoDaPack 2.0: a stand-alone, multi-platform compositional software. In: Egozcue, J.J., Tolosana-Delgado, R., Ortego, M.I. (Eds.), CoDaWork'11: 4th International Workshop on Compositional Data Analysis. Sant Feliu de Guíxols.
Da Pelo, S., Ghiglieri, G., Buttau, C., Biddau, R., Cuzzocrea, C., Funedda, A., Carletti, A., Vacca, S., Cidu, R., 2017. Coupling 3D hydrogeological modelling and geochemical mapping for an innovative approach to support management of aquifers. Ital. J. Eng. Geol. Environ. Spec. Issue 1. https://doi.org/10.4408/IJEGE.2017-01.S-04.
Daunis-I-Estadella, J., Barcelo-Vidal, C., Buccianti, A., 2006. In: Buccianti, A., Materu-Figueras, G., Pawlowsky-Glahn, V. (Eds.), Exploratory compositional data analysis. In: Compositional Data Analysis in the Geosciences: from theroy to practice. Special Publications 264, Geological Society, London, pp. 161–174.
De Vivo, B., Boni, M., Costabile, S., 1998. Baseline formational anomalies versus mining pollution: geochemical risk maps of Sardinia, Italy. J. Geochem. Explor. 64, 321–337.
Delitala, A.M.S., Cesari, D., Chessa, P.A., Ward, N., 2000. Precipitation over sardinia (Italy) during the 1946–1993 rainy seasons and associated large-scale climate variations. Int. J. Climatol. 20, 519–541.
Dill, H.G., Fricke, A., Henning, K.-H., 1995. The origin of Ba- and REE-bearing aluminium-phosphate-sulphate minerals from the Lohrheim kaolinitic clay deposit (Rheinisches Schiefergebirge, Germany). Appl. Clay Sci. 10, 231–245.
Dold, B., 2010. Basic Concepts in Environmental Geochemistry of Sulfidic Mine-Waste Management. Waste Management, Er Sunil Kumar, ISBN 978-953-7619-84-8.
EC (European Community), 2006. Council Directive 2006/118/EC, on the protection of groundwater against pollution and deterioration. Off. J, European Commission, Bruxelles.

EC (European Community), 2014. Commission Directive 2014/80/EU of 20 June 2014 amending Annex II to Directive 2006/118/EC of the European Parliament and of the Council on the protection of groundwater against pollution and deterioration. Off. J, European Commission, Bruxelles.
Edmunds, W.M., Shand, P., Hart, P., Ward, R.S., 2003. The natural (baseline) quality of groundwater: a UK pilot study. Sci. Total Environ. 310, 25–35.
Egozcue, J.J., Pawlowsky-Glahn, V., Mateu-Figueras, G., Barcelo-Vidal, C., 2003. Isometric logratio trasformations for compositional data analysis. Math. Geol. 35 (1), 280–300.
ESRI, 2013. In: Environmental Systems Research Institute, Esri. New York Street, Redlands, California 92373-8100, USA, p. 380.
Filzmoser, P., Hron, K., Reimann, C., 2009. Principal component analysis for compositional data with outliers. Environmetrics 20, 621–632.
Funedda, A., Naitza, S., Buttau, C., Cocco, F., Dini, A., 2018. Structural Controls of Ore Mineralization in a Polydeformed Basement: Field examples from the Variscan Baccu Locci Shear Zone (SE Sardinia, Italy). Minerals 8, 456. https://doi.org/10.3390/min8100456.
Funedda, A., Oggiano, G., Pasci, S., 2000. The logudoro basin: a key area for the tertiary tectono-sedimentary evolution of north sardinia. Boll. Soc. Geol. Ital. 119, 31–38.
Frau, F., Cidu, R., Ardau, C., 2012. Short-term changes in water chemistry in the Baccu Locci stream (Sardinia, Italy) affected by past mining. Appl. Geochem. 27 (9), 1844–1853.
Frau, F., Cidu, R., Casu, M., Soriga, A., 2019. Assessing arsenic sources in landfill areas: a case study in sardinia. Ital. J. Geosci. 138, 116–123. https://doi.org/10.3301/IJG.2018.30.
Ghiglieri, G., Carletti, A., Pittalis, D., 2014. Runoff coefficient and average yearly natural aquifer recharge assessment by physiography-based indirect methods for the island of Sardinia (Italy) and its NW area (Nurra). J. Hydrol. 519, 1779–1791.
Gozzi, C., Sauro, Graziano R., Buccianti, A., 2020. Part-whole relations: new insights about the dynamics of complex geochemical riverine systems. Minerals 10 (6), 501.
Gray, D., Reid, N., Noble, R., Thorne, R., Giblin, A., 2019. Hydrogeochemical mapping of the australian continent. CSIRO, Australia. EP195905, 110 pp.
Grunsky, E.C., 2010. The interpretation of geochemical survey data. Geochemistry Exploration Environment Analysis 10, 27–74.
GURI (Gazzetta Ufficiale della Repubblica Italiana), 2006. GURI (Gazzetta Ufficiale della Repubblica Italiana), 2006. Decreto legislativo 3 aprile 2006, n. 152 Norme in materia ambientale. Gazzetta Ufficiale della Repubblica Italiana n. 88 del 14-4-2006, suppl. ord. n. 96, Roma (in Italian).
GURI (Gazzetta Ufficiale della Repubblica Italiana), 2009. GURI (Gazzetta Ufficiale della Repubblica Italiana), 2009. Decreto legislativo 16 marzo 2009, n. 30. Attuazione della direttiva 2006/118/CE, relativa alla protezione delle acque sotterranee dall'inquinamento e dal deterioramento. Gazzetta Ufficiale della Repubblica Italiana n. 79 del 4-4-2009, Roma (in Italian).
GURI (Gazzetta Ufficiale della Repubblica Italiana), 2016. Decreto legislativo 6 luglio 2016. Recepimento della direttiva 2014/80/UE della Commissione del 20 giugno 2014 che modifica l'allegato II della direttiva 2006/118/CE del Parlamento europeo e del Consiglio sulla protezione delle acque sotterranee dall'inquinamento e dal deterioramento. Gazz. Uff. Rep. Ital. n. 165 del 16-7-2016, Roma (in Italian).
IMH (Italian Ministry of Health), 2016. Acque potabili. Tallio. Ministero della Salute - Direzione generale della prevenzione sanitaria (in Italian). www.salute.gov.it.
ISPRA (Istituto Superiore per la Protezione e la Ricerca Ambientale), 2018. ISPRA (Istituto Superiore per la Protezione e la Ricerca Ambientale), 2018. Linea guida per la determinazione dei valori di fondo per i suoli e per le acque sotterranee. SNPA, 08 2018, Roma (in Italian).
ISTAT (Istituto Nazionale di Statistica), 2011. Censimento della popolazione 2011. http://www.istat.it/it/sardegna. Last accessed in July 2021.
Kierczak, J., Pietranik, A., Pędziwiatr, A., 2021. Ultramafic geoecosystems as a natural source of Ni, Cr, and Co to the environment: a review. Sci. Total Environ. 755, 142620.
Langmuir, D., 1997. Aqueous Environmental Geochemistry. In: Prentice-Hall, p. 600 p..
Lee, L., Helsel, D., 2005. Baseline models of trace elements in major aquifers of the United States. Appl. Geochem. 20, 1560–1570.
Lohan, M.C., Tagliabue, A., 2018. Oceanic Micronutrients: Trace Metals that are Essential for Marine Life. Elements 14, 385–390. https://doi.org/10.2138/gselements.14.6.385.
Lorrai, M., Mereu, I., 1999. Indagine geochimica sulle acque della zona costiera di tertenia (sardegna orientale). Rend. Sem. Fac. Sci. Univ. Cagliari 69, 125–137 (in Italian).
Lustrino, M., Fedele, L., Melluso, L., Morra, V., Ronga, F., Geldmacher, J., Duggen, S., Agostini, S., Cucciniello, C., Franciosi, L., Meisel, T., 2013. Origin and evolution of Cenozoic magmatism of Sardinia (Italy). A combined isotopic (Sr–Nd–Pb–O–Hf–Os) and petrological view. Lithos 180–181, 138–158.
Mameli, P., Mongelli, G., Oggiano, G., Dinelli, E., 2007. Mineralogy and geochemistry of the nurra bauxites (western sardinia): constraints for the conditions of the formation and parental affinity. Int. J. Earth Sci. 96, 887–902.
Marcello, A., Mazzella, A., Naitza, S., Pretti, S., Tocco, S., Valera, P., Valera, R., 2008. Carta metallogenica e delle georisorse della sardegna, scala 1: 250,000. Litografia artistica e cartografica S.r.l, Firenze (in Italian).
Martin-Fernandez, J.A., Hron, K., Templ, M., Filzmoser, P., Palarea-Albaladejo, J., 2015. Bayesian-multiplicative treatment of count zeros in compositional data sets. Stat. Model. 15 (2), 134–158.
Matschullat, J., Ottenstein, R., Reimann, C., 2000. Geochemical background - can we calculate it? Environ. Geol. 39, 990–1000.
Mongelli, G., Mameli, P., Sinisi, R., Buccione, R., Oggiano, G., 2021. Rees and other critical raw materials in cretaceous mediterranean-type bauxite: the case of the Sardinian ore (Italy). Ore Geol. Rev. 139, 1–15.
Mormone, A., Piochi, M., 2020. Mineralogy, Geochemistry and Genesis of Zeolites in Cenozoic Pyroclastic Flows from the Asuni Area (Central Sardinia, Italy). Minerals 10, 268.
Moroni, M., Naitza, S., Ruggieri, G., Aquino, A., Costagliola, P.De, Giudici, G., Caruso, S., Ferrari, E., Fiorentini, M.L., Lattanzi, P., 2019. The Pb-Zn-Ag vein system at montevecchio-ingurtosu, southwestern sardinia, Italy: a summary of previous knowledge and new mineralogical, fluid inclusion, and isotopic data. Ore Geol. Rev. 115, 103194.
Naitza, S., Conte, A.M., Cuccuru, S., Oggiano, G., Secchi, F., Tecce, F., 2017. A late Variscan tin province associated to the ilmenite-series granites of the Sardinian Batholith (Italy): the Sn and Mo mineralisation around the Monte Linas ferroan granite. Ore Geol. Rev. 80, 1259–1278.
Nordstrom, D.K., 2015. Baseline and premining geochemical characterization of mined sites. Appl. Geochem. 57, 17–34.
Oorts, K., Schoeters, I., 2014. Use of monitoring data for risk assessment of metals in soil under the European REACH regulation. In: Reimann, C., Birke, M., Demetriades, A., Filzmoser, P., O'Connor, P. (Eds.), Chemistry of Europe's Agricultural Soils – Part B: General Background Information and Further Analysis of the GEMAS Data Set. Geologisches Jahrbuch (Reihe B103), Schweizerbarth, Hannover (2014), pp. 189–202.
Palomba, M., Padalino, G., Marchi, M., 2006. Industrial mineral occurrences associated with Cenozoic volcanic rocks of Sardinia (Italy): Geological, mineralogical, geochemical features and genetic implications. Ore Geol. Rev. 29, 118–145.
Parrone, D., Ghergo, S., Preziosi, E., 2019. A multi-method approach for the assessment of natural background levels in groundwater. Sci. Total Environ. 659, 884–894.
Parviainen, A., Loukola-Ruskeeniemi, K., 2019. Environmental impact of mineralised black shales. Earth Sci. Rev. 192, 65–90.
Paternoster, M., Oggiano, G., Sinisi, R., Caracausi, A., Mongelli, G., 2017. Geochemistry of two contrasting deep fluids in the Sardinia microplate (western Mediterranean): Relationships with tectonics and heat sources. J. Volcanol. Geotherm. Res. 336, 108–117.
Pawlowsky-Glahn, V., Buccianti, A., 2011. Compositional data analysis: theory and applications. John Wiley & Sons.
Plumlee, G.S., 1999. The environmental geology of mineral deposits. In: Plumlee, G.S., Logsdon, M.J. (Eds.), The Environmental Geochemistry of Mineral Deposits, Part a. Society of Economic Geologists, Littleton, CO, pp. 71–116.
RAS, 2005. Deliberazione della Giunta Regionale n. 1/12 del 18/01/2005 con cui la Regione Sardegna ha designato, quale zona vulnerabile da nitrati di origine agricola (ZVN), una porzione del territorio del Comune di Arborea. Regione Autonoma della Sardegna, Cagliari (in Italian).
RAS, 2006. Piano di tutela delle acque (regional plan for the water protection). Regione Autonoma della Sardegna, Cagliari (in Italian).
RAS, 2011. Caratterizzazione, obiettivi e monitoraggio dei corpi idrici sotterranei della Sardegna approvato con Deliberazione della Giunta Regionale n. 1/16 del 14/01/2011. Regione Autonoma della Sardegna Cagliari (in Italian, last accessed in August 2021). https://www.regione.sardegna.it/documenti/1_328_20130906131252.zip.
RAS, 2013. Carta geologica di base della Sardegna. Regione Autonoma della Sardegna, Cagliari (Last accessed in October 2021). http://www.sardegnageoportale.it/argomenti/cartageologica.html.
R Development Core Team, 2013. R: a language and environment for statistical computing. R Foundation for Statistical Computing, Vienna, Austria http://www.Rproject.org/.
Reimann, C., Birke, M., Demetriades, A., Filzmoser, P., O'Connor, P., 2014. In: Chemistry of Europe's Agricultural Soils - Part A: Methodology and Interpretation of the GEMAS Data Set, Geologisches Jahrbuch (Reihe B 102). Schweizerbarth, Hannover, p. 528.
Reimann, C., Birke, M., Demetriades, A., Filzmoser, P., O'Connor, P., 2014. In: Chemistry of Europe's Agricultural Soils - Part B: General Background Information and Further Analysis of the GEMAS Data Set, Geologisches Jahrbuch (Reihe B 103). Schweizerbarth, Hannover, p. 352.
Reimann, C., de Caritat, P., 2017. Establishing background variation and threshold values for 59 elements in australian surface soil. Sci. Total Environ. 578, 633–648.
Reimann, C., Fabian, K., Birke, M., Filzmoser, P., Demetriades, A., Negrel, P., Oorts, K., Matschullat, J., de Caritat, P., The GEMAS Project Team., 2018. GEMAS: Establishing geochemical background and threshold for 53chemical elements in European agricultural soil. Applied Geochemistry 88, 302–318.
Reimann, C., Filzmoser, P., Fabian, K., Hron, K., Birke, M., Demetriades, A., Dinelli, E., Ladenberger, A., 2012. The concept of compositional data analysis in practice - total major element concentrations in agricultural and grazing land soils of Europe. Sci. Total Environ. 426, 196–210.
Reimann, C., Filzmoser, P., Garrett, R.G., Dutter, R., 2008. In: Statistical Data Analysis Explained: Applied Environmental Statistics with. R. John Wiley & Sons, Ltd., ISBN 978-0-470-98581-6, p. 362
Reimann, C., Garrett, R.G., Filzmoser, P., 2005. Background and threshold - critical comparison of methods of determination. Sci. Total Environ. 346, 1–16.
Rudnick, R.L., Gao, S., 2014. Composition of the continental crust. Treatise on. Geochemistry. https://doi.org/10.1016/B978-0-08-095975-7.00301-6.
Ryan, J.G., Langmuir, C.H., 1993. The systematics of boron abundances in young volcanic rocks. Geochim. Cosmochim. Acta 57, 1489–1498.
Sahoo, P.K., Dall'Agnol, R., Salomão, G.N., da Silva Ferreira Junior, J., et al., 2019. High resolution hydrogeochemical survey and estimation of baseline concentrations of trace elements in surface water of the Itacaiúnas River Basin, southeastern Amazonia: Implication for environmental studies. J. Geochem. Explor. 205, 106321.
Simeone, R., Dilles, J.H., Padalino, G., Palomba, M., 2005. Mineralogical and stable isotope studies of kaolin deposits: shallow epithermal systems of western Sardinia, Italy. Econ. Geol. 100, 115–130.

Sinisi, R., Mameli, P., Mongelli, G., Oggiano, G., 2012. Different Mn-ores in a continental arc setting: Geochemical and mineralogical evidences from Tertiary deposits of Sardinia (Italy). Ore Geol. Rev. 47, 110–125.
Shumway, R.H., Azari, R.S., Kayhanian, M., 2002. Statistical approaches to estimating mean water quality concentrations with detection limits. Environ. Sci. Technol. 36, 3346–3353.
Smith, D.B., Cannon, W.F., Woodruff, L.G., Ellefsen, K.J., 2014. In: Geochemical and Mineralogical Maps for Soils of the Conterminous United States, p. 386.
Stumm, W., Morgan, J.J., 1996. Aquatic chemistry, chemical equilibria and rates in natural waters, Third edition. John Wiley & Sons Inc., New York.
Verboven, S., Hubert, M., 2005. LIBRA: a MATLAB library for robust analysis. Chemom. Intell. Lab. Syst. 75, 127–136.
WHO, 2017. Guidelines for drinking-water quality: fourth edition incorporating the first addendum. World Health Organization, Geneva, ISBN 978-92-4-154995-0.
Wright, M.T., Belitz, K., 2010. Factors controlling the regional distribution of vanadium in groundwater. Ground Water 48, 515–525.
Zanotti, C., Caschetto, M., Bonomi, T., Parini, M., Cipriano, G., Fumagalli, L., Rotiroti, M., 2022. Linking local natural background levels in groundwater to their generating hydrogeochemical processes in Quaternary alluvial aquifers. Sci. Total Environ. 805, 150259.
Zoback, M.L., 2001. Grand challenges in earth and environmental sciences - science, stewardship, and service for the twenty-first century. Geol. Soc. Am. Today 11 (12), 41–47.